Chaos, Solitons and Fractals 153 (2021) 111473

Contents lists available at ScienceDirect

Chaos, Solitons and Fractals

Nonlinear Science, and Nonequilibrium and Complex Phenomena

journal homepage: www.elsevier.com/locate/chaos

Frontiers

K-Narayana sequence self-Similarity. flip graph views of k-Narayana self-Similarity☆

Engin Özkan[a], Bahar Kuloğlu[b], James F. Peters[c,d,*]

[a] Department of Mathematics, Faculty of Arts and Sciences, Erzincan Binali Yıldırım University, Erzincan, Turkey
[b] Graduate School Of Natural And Applied Sciences, Erzincan Binali Yıldırım University, Erzincan, Turkey
[c] Computational Intelligence Laboratory, University of Manitoba, WPG, MB, R3T 5V6, Canada
[d] Department of Mathematics, Faculty of Arts and Sciences, Adiyaman University, Adiyaman 02040, Turkey

ARTICLE INFO

Article history:
Received 29 May 2021
Revised 19 September 2021
Accepted 22 September 2021

2010 MSC:
11B39
05C10,

Keywords:
Flip graphs
K-Narayana sequence
Pascal 3-triangle
Planar graph
Self-Similarity

ABSTRACT

This paper introduces self-similarity inherent in planar Milich-Jennings centered flip graphs derived from the Narayana sequence. We show that self-similarity found in a Narayana sequence yields a connected spanning subgraph with a centered flip. This paper has several main results (1) Every Narayana sequence constructs a flip graph, (2) Every Narayana sequence is self-similar and (3) Every Pascal 3-triangle has a free group presentation.

© 2021 Elsevier Ltd. All rights reserved.

1. Introduction

In this paper, both population growth as well as population decline are represented by the bipolar form of the Narayana sequence, namely,

$$\ldots, -13, -9, -6, -4, -3, -2, -1, -1, -1, 0, 1, 1, 1, 2, 3, 4, 6, 9, 13, \ldots$$

There is an inherent self-similarity in Narayana sequences (see, *e.g.*, the partial plot of three different forms of this sequence shown in Fig. 1.

For the k^{th} member N_k of a population, the Narayana growth model is defined by the linear recurrence sequence $N_k = N_{k-1} + N_{k-3}, k \geq 3$, starting with $N_0, N_1, N_2, N_3 = 0, 1, 1, 1$ representing 3 generations that starts growing at $N_3 = N_2 + N_0 = 1 + 1 = 2$. This population growth model was introduced 1356 by Nārāyana Paṇḍita [1]. Similarly, this sequence has a population decline model defined by $N_k = N_{k-1} + N_{k-3}, k \leq -3$, starting with $N_0, N_{-1}, N_{-2}, N_{-3} = 0, -1, -1, -1$ representing 3 declining generations that starts declining at $N_{-4} = N_{-1} + N_{-3} = -1 + (-1) = -2$.

The self-similarity in Fig. 1 is a result of considering the generalized Narayana sequence [2] defined by

$$\begin{aligned} N_{k,n} &= kN_{k,n-1} + N_{k,n-3}, n \geq 0, k \geq 3 \\ &= 0, 1, 1, 1, 2, 3, 4, 6, 9, 13, \end{aligned}$$

with the initial values $N_{k,0} = 0, N_{k,1} = 1$ and $N_{k,2} = k$, yielding the sequence $0, 1, k, k^2, k^3 + 1, k^4 + 2k, k^5 + 3k^2$. In the study of Narayana sequence self-similarity, we consider $\pm N_{k,n}, k \geq 3$, representing population growth as well as population decline.

It is well-known graph self-similarity such that shown for $\pm N_{k,n}$ in Fig. 1 leads to generalizations of self-similarity [3, §4.4,p. 120]. From the edges in graph similarity, it is possible to construct examples of border (outline) fractals [3, §6.1].

A flip graph is a form of undirected, simple graph, which we consider next in a closer look at bipolar Narayana sequences and their self-similarities. A **simple graph** is an undirected graph on a finite set of vertexes without loops. A flip graph is constructed by flipping selected chords spanning the vertices in the triangulation of a collection of vertices.

Example 1. Sample flipped chords in a triangulation is shown in Fig. 2. The flipping of a chord is a natural occurrence in tracing the self-similar behavior of the growth and its companion decline

☆ Self-similarity inherent in flip graph views of the k-Narayana Sequence.

* Corresponding author.
E-mail address: james.peters3@umanitoba.ca (J.F. Peters).

https://doi.org/10.1016/j.chaos.2021.111473
0960-0779/© 2021 Elsevier Ltd. All rights reserved.

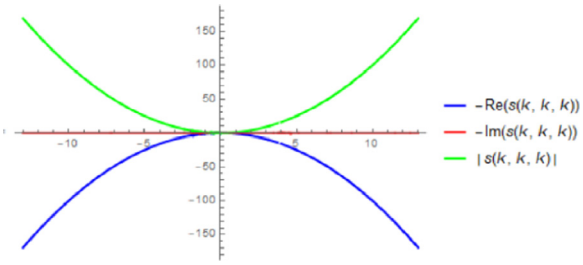


Fig. 1. Narayana population growth & decline plot over $[-13, 13]$.

represented by vertexes that correspond to a new birth or a new death in bipolar Narayana sequence.

Motivation for Flig-graph Realizations of bipolar Narayana sequences. This paper introduces the use of Milich-Jennings flip graphs [4],[5, §2.1.2] in representing the bipolarity of Narayana sequences. The main motivation for considering flip graphs is its concise as well as visual rendition of self-similarity inherent in Narayana population growth as well as population decline. The hills and valleys in a Narayana flip also call attention to the shape of a bipolar Narayana sequence.

The self-similarity of the Narayana sequence $\pm N_{k,n}$ introduced in this paper leads to the following result. **Theorem** Every Narayana sequence is self-similar.

Remark 1. For the details, see Theorem 1.1, Section 2.

2. Preliminaries

In this section the construction of self-similar graphs via bipolar Narayana sequences. A **bipolar Narayana sequence** $\pm N_{k,n}$ represents two extremes, namely, the growth of a population at one extreme and the decline of a population at the other extreme, representable in a planar self-similar graph.

This paper also considers Pascal-like triangles [6] with corresponding finite cyclic group presentations derived from k-Narayana sequences.

Definition 1. [4,7] A planar **flip graph** is a 2D graph whose vertexes represent combinatorial objects of interest and an edge between any two objects that differ only by a small change operation called a *flip*.

Example 2. A flip graph representing the beginning of a population and its decline is shown in Fig. 3.1. This flip graph exhibits the simplest form self-similarity centered at the origin, *i.e.*, -2,-1-1,-1,0,1,1,1,2. The altitude 2 to the right of the origin represents the initial population. The altitude 2 to the left of the origin represents the initial decline of the same population.

Example 3. A flip graph representing the beginning of a population and its decline is shown in Fig. 3.2. This flip graph exhibits 4th generation self-similarity centered at the origin, *i.e.*, -6-4,-3,-2,-1-1,-1,0,1,1,1,2,3,4,6. The altitudes 2,3,4,6 to the right of the origin represent initial population growth. The altitudes 2,3,4,6 to the left of the origin represents the initial decline of the same population.

Remark 2. Positive altitudes to the left of the origin in Figs. 3.1 and 3.2 represent the count of those generations in a population that failed to appear.

Lemma 1. *A bipolar Narayana sequence constructs a flip graph.*

Proof. Let $\pm N_{k,n}$ be a bipolar Narayana sequence. We start with $k = \pm 3$ with three vertexes, namely, vertexes at $\pm 1, \pm 3$ on the horizontal axis and a vertexes at (3,2), (-3,2), which we triangulate. The edge from (1,0) to (3,2) represents a small change (a flip) in population growth, which contrasts another flip along the edge from (-1,0) to (-3,2). Continuing this triangulation on additional triple vertexes derived from a Narayana sequence constructs a flip graph. □

Theorem 1. *Every bipolar Narayana sequence is self-similar.*

Proof. From what has been observed about the relationship between self-similarity and flip graphs and from Lemma 1, the result follows. □

Remark 3. From Theorem 1, we obtain a natural basis for a free group presentation of the flip graph for a Narayana sequence. That is, a flip graph viewed as a pair of cycles along the edges of the triangles in the graph makes it possible to travel in either the positive or negative direction. In effect, every $+^{ve}$ traversal a to the right in a Narayana flip graph has a corresponding $-^{ve}$ traversal $-a$ to the left, giving us inverse elements, which sum to zero, $a - a = 0$. For more about this, see Section 5 and Appendix C.

The k-Narayana numbers are given by Binets formula Eq. (1).

$$N_{k,n} = \frac{\alpha_k^{n+1}}{(\alpha_k - \beta_k)(\alpha_k - \gamma_k)} + \frac{\beta_k^{n+1}}{(\beta_k - \alpha_k)(\beta_k - \gamma_k)} + \frac{\gamma_k^{n+1}}{(\gamma_k - \beta_k)(\gamma_k - \alpha_k)} \tag{1}$$

where

$$\alpha_k = \frac{1}{3}\left(k + k^2 \sqrt[3]{\frac{2}{27 + 2k^3 + 3\sqrt{81 + 12k^3}}} + \sqrt[3]{\frac{27 + 2k^3 + 3\sqrt{81 + 12k^3}}{2}}\right).$$

$$\beta_k = \frac{1}{3}\left(k - wk^2 \sqrt[3]{\frac{2}{27 + 2k^3 + 3\sqrt{81 + 12k^3}}} + w^2 \sqrt[3]{\frac{27 + 2k^3 + 3\sqrt{81 + 12k^3}}{2}}\right).$$

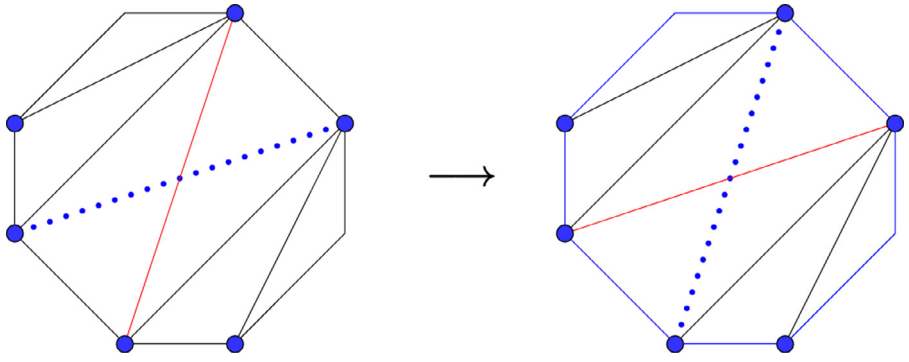
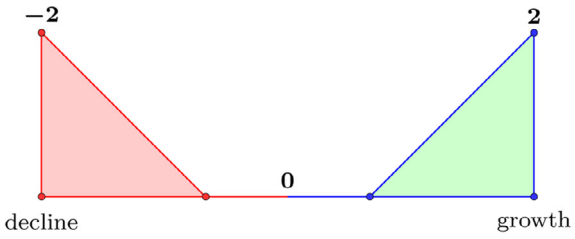
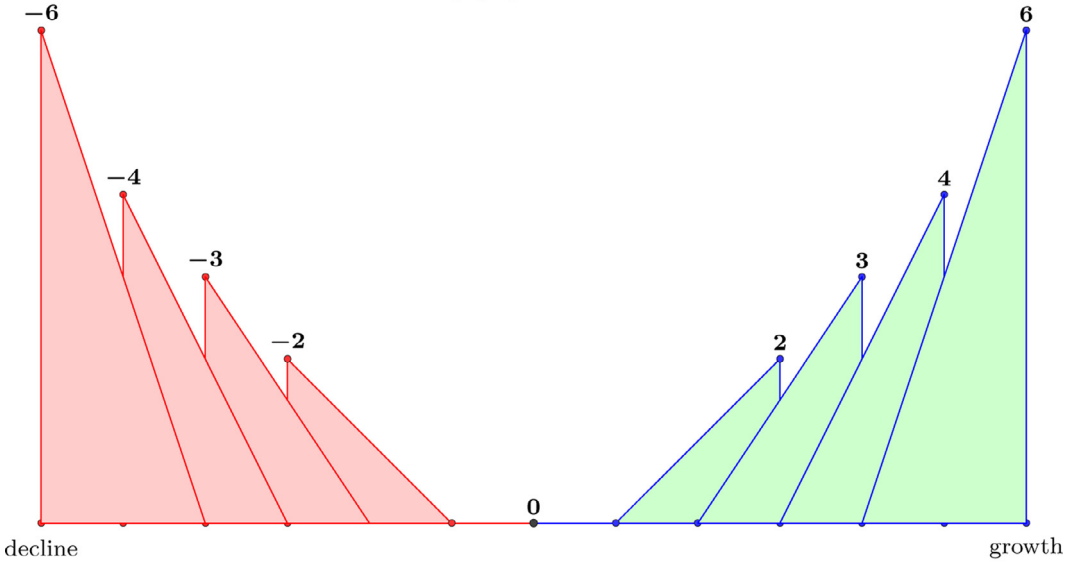


Fig. 2. Flipped Chord in a Triangulation.



3.1: initial flip graph



3.2: flip graph over -6,-4,-3,-2,...,0...,2,3,4,6

Fig. 3. Narayana flip graphs.

$$\gamma_k = \frac{1}{3}\left(k + w^2k^2\sqrt[3]{\frac{2}{27+2k^3+3\sqrt{81+12k^3}}} + w\sqrt[3]{\frac{27+2k^3+3\sqrt{81+12k^3}}{2}}\right).$$

$w = \frac{1+i\sqrt{3}}{2}$ is the primitive cube root of unity [2]. Characteristic equation of these numbers is Eq. (2)

$$x^3 + kx^2 - 1 = 0 \tag{2}$$

For any integer number k, $k \neq 0$, we have

$$Q_k = \begin{pmatrix} k & 0 & 1 \\ 1 & 0 & 0 \\ 0 & 1 & 0 \end{pmatrix}$$

and for $n \geq 3$,

$$(Q_k)^n = \begin{pmatrix} N_{k,n+1} & N_{k,n-1} & N_{k,n} \\ N_{k,n} & N_{k,n-2} & N_{k,n-1} \\ N_{k,n-1} & N_{k,n-3} & N_{k,n-2} \end{pmatrix}$$

Then Q_k is a generating matrix of the k-Narayana sequence [2].

3. The k-Narayana numbers and properties

Theorem 2. *[Cassini's Identity]*

$$N_{k,n-1}N_{k,n+1} - N_{k,n}^2 = -N_{k,-n-1}.$$

Proof. By using the Binets formula, we get

$$\left(\frac{\alpha_k^n}{(\alpha_k-\beta_k)(\alpha_k-\gamma_k)} + \frac{\beta_k^n}{(\beta_k-\alpha_k)(\beta_k-\gamma_k)} + \frac{\gamma_k^n}{(\gamma_k-\beta_k)(\gamma_k-\alpha_k)}\right)$$
$$\left(\frac{\alpha_k^{n+2}}{(\alpha_k-\beta_k)(\alpha_k-\gamma_k)} + \frac{\beta_k^{n+2}}{(\beta_k-\alpha_k)(\beta_k-\gamma_k)} + \frac{\gamma_k^{n+2}}{(\gamma_k-\beta_k)(\gamma_k-\alpha_k)}\right)$$
$$-\left(\frac{\alpha_k^{n+1}}{(\alpha_k-\beta_k)(\alpha_k-\gamma_k)} + \frac{\beta_k^{n+1}}{(\beta_k-\alpha_k)(\beta_k-\gamma_k)} + \frac{\gamma_k^{n+1}}{(\gamma_k-\beta_k)(\gamma_k-\alpha_k)}\right)^2$$
$$= \frac{\alpha_k^n\beta_k^{n+2} - 2\alpha_k^{n+1}\beta_k^{n+1} + \alpha_k^{n+2}\beta_k^n}{(\alpha_k-\beta_k)(\alpha_k-\gamma_k)(\beta_k-\alpha_k)(\beta_k-\gamma_k)}$$
$$+ \frac{\alpha_k^n\gamma_k^{n+2} - 2\alpha_k^{n+2}\gamma_k^n + \alpha_k^{n+2}\gamma_k^n}{(\alpha_k-\beta_k)(\alpha_k-\gamma_k)(\gamma_k-\alpha_k)(\gamma_k-\beta_k)}$$
$$+ \frac{\beta_k^n\gamma_k^{n+2} - 2\beta_k^{n+1}\gamma_k^{n+1} + \beta_k^{n+2}\gamma_k^n}{(\beta_k-\alpha_k)(\beta_k-\gamma_k)(\gamma_k-\alpha_k)(\gamma_k-\beta_k)}$$
$$= \frac{\alpha_k^n\beta_k^n(\alpha_k-\beta_k)^2}{(\alpha_k-\beta_k)(\alpha_k-\gamma_k)(\beta_k-\alpha_k)(\beta_k-\gamma_k)}$$
$$+ \frac{\alpha_k^n\gamma_k^n(\alpha_k-\gamma_k)^2}{(\alpha_k-\beta_k)(\alpha_k-\gamma_k)(\gamma_k-\alpha_k)(\gamma_k-\beta_k)}$$
$$+ \frac{\beta_k^n\gamma_k^n(\beta_k-\gamma_k)^2}{(\gamma_k-\alpha_k)(\gamma_k-\beta_k)(\beta_k-\alpha_k)(\beta_k-\gamma_k)}$$
$$= -\left(\frac{\alpha_k^n\beta_k^n}{(\alpha_k-\gamma_k)(\beta_k-\gamma_k)} + \frac{\alpha_k^n\gamma_k^n}{(\alpha_k-\beta_k)(\gamma_k-\beta_k)} + \frac{\beta_k^n\gamma_k^n}{(\beta_k-\alpha_k)(\gamma_k-\alpha_k)}\right)$$

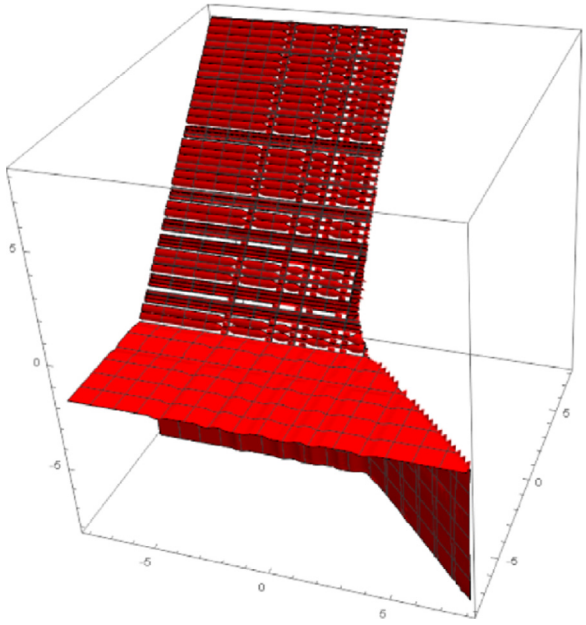


Fig. 4. 3D flip graph of Narayana population growth & decline.

$$= -\left(\frac{\gamma_k^{-n}}{(\alpha_k-\gamma_k)(\beta_k-\gamma_k)} + \frac{\beta_k^{-n}}{(\alpha_k-\beta_k)(\gamma_k-\beta_k)} + \frac{\alpha_k^{-n}}{(\beta_k-\alpha_k)(\gamma_k-\alpha_k)}\right)$$

$$= -N_{k,-n-1}$$

□

Remark 4. A 3D flip graph exhibiting the self-similarity of the Narayana sequence using Binet's formula is shown in Fig. 4.

Theorem 3.

$$\lim_{n\to\infty}\frac{N_{k,n}}{N_{k,n-1}} = \alpha_k$$

Proof. Symmetric with the proof of Theorem 2. □

Theorem 4. *For any integer $n \geq 2$, we have*

$$\alpha_k^{n+3} = k\alpha_k^{n+2} + 1.$$
$$\beta_k^{n+3} = k\beta_k^{n+2} + 1.$$
$$\gamma_k^{n+3} = k\gamma_k^{n+2} + 1.$$

where $\alpha_k, \beta_k, \gamma_k$ are the roots of the characteristic Eq. 2.

Proof. Since $\alpha_k, \beta_k, \gamma_k$ are the roots of the characteristic Eq. (2) then

$$\alpha_k^{n+3} = k\alpha_k^{n+2} + 1$$

$$\beta_k^{n+3} = k\beta_k^{n+2} + 1$$

$$\gamma_k^{n+3} = k\gamma_k^{n+2} + 1$$

multiplying both sides of these equations by α_k^n, β_k^n and γ_k^n respectively, we obtain the desired result. □

Theorem 1. *For any integer $n \geq 0$, we write*

$$\sum_{i=0}^{n} k^i N_{k,2i} = 0.$$

Proof. Symmetric with the proof of Theorem 2. □

Theorem 5. *For $n \geq 3$, we have*

$$\begin{vmatrix} N_{k,n+1} & N_{k,n-1} & N_{k,n} \\ N_{k,n} & N_{k,n-2} & N_{k,n-1} \\ N_{k,n-1} & N_{k,n-3} & N_{k,n-2} \end{vmatrix} = 1$$

Proof. If we are making some algebraic operation:

$$N_{k,n+1}^3 + N_{k,n}^3 + N_{k,n-1}^3 - 2N_{k,n+1}^2 N_{k,n} + N_{k,n}^2 N_{k,n+1} + N_{k,n+1}N_{k,n-1}^2$$

$$+ N_{k,n}^2 N_{k,n-1} - 3N_{k,n-1}N_{k,n+1}N_{k,n} = 1$$

We get the equation.

For example, $n = 3$, we have

$$\begin{vmatrix} N_{k,4} & N_{k,2} & N_{k,3} \\ N_{k,3} & N_{k,1} & N_{k,2} \\ N_{k,2} & N_{k,0} & N_{k,1} \end{vmatrix} = \begin{vmatrix} k^3+1 & k & k^2 \\ k^2 & 1 & k \\ k & 0 & 1 \end{vmatrix} = 1$$

□

Similarly, we obtain the following result.

Theorem 6 (Sum of first terms)**.** . *Let $S_{k,n}$ be the sum of the first $(n+1)$ terms of the k-Narayana sequence, that is*

$$S_{k,n} = \sum_{i=0}^{n} N_{k,i}.$$

Then

$$S_{k,n} = \frac{N_{k,1} + N_{k,n} + N_{k,n+1} + N_{k,n+2}}{k} - N_{k,n+1}.$$

4. The pascal 3-triangle

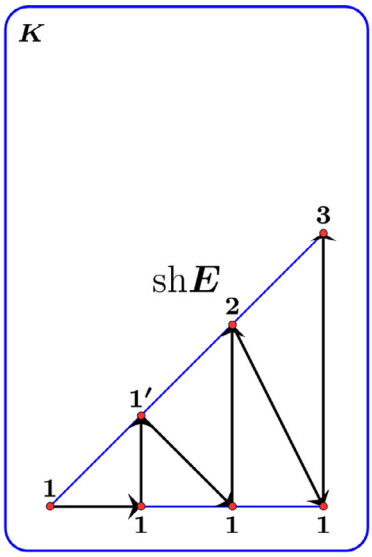
We deduce the value of any k-Narayana number by simple substitution on the corresponding $N_{k,n}$. The sequence $N_{1,n}$ is the classical Narayana sequence. By the definition of the k-Narayana numbers [2], the first of them are:

$$N_{k,1} = 1$$
$$N_{k,2} = k$$
$$N_{k,3} = k^2$$
$$N_{k,4} = k^3 + 1$$
$$N_{k,5} = k^4 + 2k$$
$$N_{k,6} = k^5 + 3k^2$$
$$N_{k,7} = k^6 + 4k^3 + 1$$
$$N_{k,8} = k^7 + 5k^4 + 3k$$
$$N_{k,9} = k^8 + 6k^5 + 6k^2$$
$$N_{k,10} = k^9 + 7k^6 + 10k^3 + 1$$

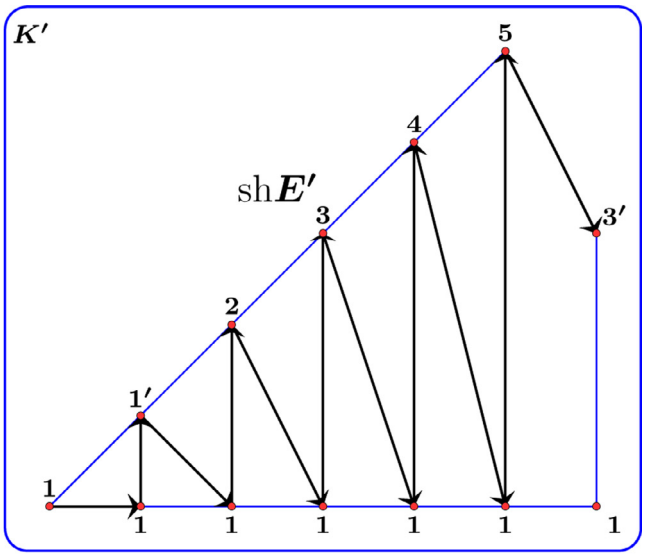
It is worth to be noted that the obtained coefficients can be written in a triangular position, in this way that every side of the triangle is triple, and for this reason this triangle has been called Pascal 3-triangle. See Table 1.

5. Free group presentation of a pascal 3-Triangle

This section introduces free group presentations that correspond to Pascal 3-triangles in a planar CW space. Briefly, a planar CW space is a collection of cells in a finite, bounded region of the Euclidean plane. A *cell* in the Euclidean plane is either a 0-cell (vertex K_0) or 1-cell (edge K_1) or 2-cell (filled triangle K_2). A **cell complex** is a collection cells attached to each other by 0- or 1-cells or by having one or more common cells. A nonvoid collection of cell complexes K has a *Closure finite Weak* (CW) topology, provided K is Hausdorff (every pair of distinct cells is contained



5.1: Pascal 3-triangle nested cycles $1,1;1',2;1,3,$ forming shape sh$\boldsymbol{E}$



5.2: Pascal 3-triangle nested cycles $1,1;1',2;1,3;1,4,1;1,5,3',$ forming planar shape sh$\boldsymbol{E'}$

Fig. 5. Pascal 3-triangle Nested Cycle Shapes sh$\boldsymbol{E}$, sh$\boldsymbol{E}'$.

Table 1
The Pascal 3-triangle.

				1						
				1						
				1						
			1		1					
			1		2					
			1		3					
		1		4		1				
		1		5		3				
		1		6		6				
	1		7		10		1			
	1		8		15		4			
	1		9		21		10			
...		...		...		...		...		

in disjoint neighborhoods [8, §5.1, p. 94]) and the collection of cell complexes in K satisfy the Whitehead [9, pp. 315–317] conditions, namely, containment (the closure of each cell complex is in K) and intersection (the nonempty intersection of cell complexes is in K) (for the details, see App. Appendix A).

Pascal 3-triangles like those in Table 1 form collections of nested cycles.

Example 4. A pair of Pascal 3-triangle cycles are shown in Fig. 5, namely,

1^o Pascal 3-triangle in Fig. 5a with 3 nested cycles: 1,1;1,2;1,3. The leftmost single vertex labelled 1 in Fig. 5a is a cycle that spins on itself (this single vertex represents traversal back to 1 for each of the three cycles shown). The Pascal 3-triangle 1;1,1 in Fig. 5a forms a triangle cycle. The Pascal 3-triangle 1;1,1;1,2;1,3 in Fig. 5a forms a collection of nested cycles.

2^o Next, the Pascal 3-triangle in Fig. 5a is attached to 1,4,1;1,5,3 to form an expanded collection of nested cycles shown in Fig. 5b.

Notice that the pair of collections of nested cycles derived from Pascal 3-triangles form a pair of distinct shapes, namely, shape sh$E$ in Fig. 5a and shape shE' in Fig. 5b. The boundary of sh$E$ is denoted by bdy(sh$E$) (represented by its vertexes). Each of these shapes has a distinct boundary, which is a source of generators of a free group presentation derived from a Pascal 3-triangle. For the details concerning CW shape complexes, see App. Appendix B.

Example 5. The pair of Pascal 3-triangle nested cycles form planar shapes as shown in Fig. 5, namely,

1^o Shape sh$E$ in Fig. 5a with

Boundary in Fig. 5a bdy(sh$E$) $= \{1, 1', 2, 3\}$, limited to the upper boundary vertexes of sh$E$.

- 2^o Shape shE' in Fig. 5b with

Boundary in Fig. 5b bdy(shE') $= \{1, 1', 2, 3, 4, 5, 3'\}$, limited to the upper boundary vertexes of shE'.

Theorem 7. *Every Pascal 3-triangle has a free group presentation.*

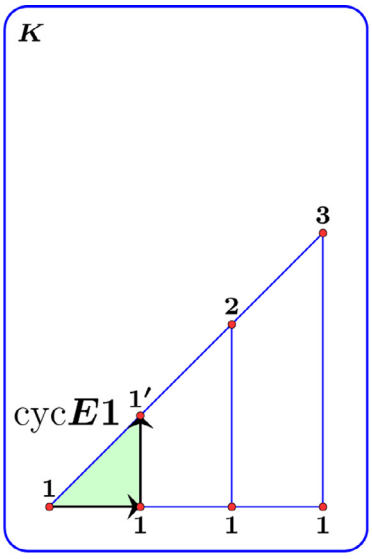
Proof. From Theorem 9 in App. Appendix C, every shape boundary is a 1-cycle CW space K (see, *e.g.*, Fig. 5a) and in the CW space K' (see, *e.g.*, Fig. 5b) has finitely-generated cyclic group presentation. □

Example 6. Each of the collections of nested cycles in Fig. 6 has an Abelian group presentation, *e.g.*,

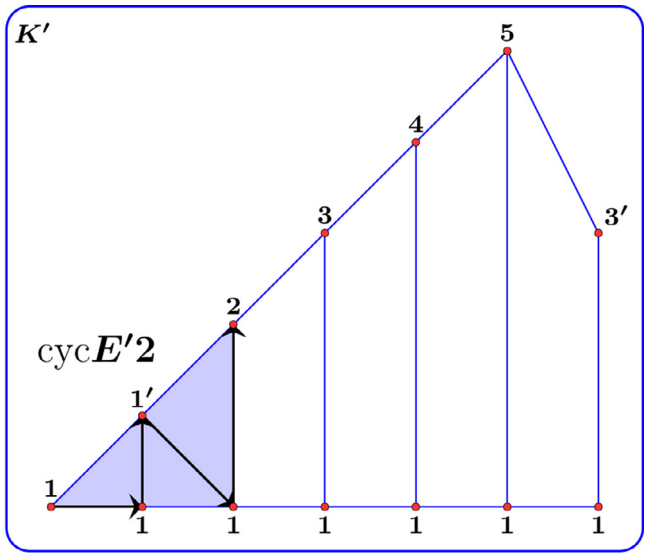
1^o Cycle cyc$\boldsymbol{E1}$ in Fig. 6a is represented by $G(\langle 1\prime\rangle, +)$ with 1 as the generator, *i.e.*, every vertex in the cycle can be reached from vertex1$\prime$.

2^o Cycle cyc$\boldsymbol{E'2}$ in Fig. 6b is represented by $G(\langle 2\rangle, +)$ with 2 as the generator, *i.e.*, every vertex in the cycle can be reached from vertex 2.

From Theorem 10 in App. Appendix C, a Pascal 3-triangle leads to a collection of nested cycles in the CW space in K (Fig. 5a) and in the CW space in K' (Fig. 5b), each of which as a free group presentation.



6.1: Pascal 3-triangle cycle $1, 1; 1'$, forming cycle cyc$E1$



6.2: Pascal 3-triangle cycles $1, 1; 1', 2,$ forming planar cycle cyc$E2$

Fig. 6. Pasal 3-triangle Cycles cyc$E1$, cyc$E'2$.

Motivation for free group presentation of Narayana sequences. This paper introduces the use of free group presentations of the cycles inherent a Narayana sequence. The main motivation for considering free groups is that it leads to Betti numbers that offer a greatly simplified view of Narayana population growth. From Theorem 7, we know that Pascal 3-triangle has a free group presentation. We observe that every segment of Narayana growth (from its beginning to its current state) has a corresponding collection of Pascal 3-triangle cycles as in Fig. 6. This means the underlying complex free group structure of Narayana growth can represented simply as a sequence of increasing Betti numbers. See Example 7 for a sample Betti number. A **Betti number** is a count of the number of generators for a free group. Instead of considering a free group presentation of Pascal 3-triangle cycles in Narayana population growth in Example 7, we obtain a simplified view of a particular stage in Narayana growth with a Betti number equaling 6. For more about this, see Appendix Appendix C.

Example 7. Each of the collections of nested cycles in Fig. 5 has a free group presentation, *e.g.*,

1º The collection of nested cycles in sh$E$ in Fig. 5a is represented by $G(\langle 1\prime, 2, 3\rangle, +)$ with vertexes1′,2,3 as the generators, *i.e.*, every vertex in the cycle can be reached from vertexes1′,2,3.

2º The collection of nested cycles in shE' in Fig. 5b is represented by $G(\langle 1\prime, 2, 3, 4, 5, 3'\rangle, +)$ with vertexes1′,2,3,4,5,3' as the generators, *i.e.*, every vertex in the cycle can be reached from vertexes1′,2,3,4,5,3'. Hence, the Betti number for this free group equals 6.

6. Views and properties of the pascal 3-triangle

Let us examine two points on x and y lines in an orthogonal coordinate system. One can see clearly, a way between an x-point and a y-point is not inverting way in the first sestet from x to y by horizontal and vertical unit section. For instance, there are four way from the point $x = (3, 0)$ to the point $y = (0, 1)$:

$\{(3,0)(2,0)(1,0)(0,0)(0,1)\}$

$\{(3,0)(2,0)(1,0)(1,1)(0,1)\}$

$\{(3,0)(2,0)(2,1)(1,1)(0,1)\}$

$\{(3,0)(3,1)(2,1)(1,1)(0,1)\}$

The number of ways between an x-point and a y-point can be seen on diagonals in Pascal 3-triangle. In Table 2, each element is obtained the sum of the elements on previous row from the left to element above.

For example, number 21 in the third row is the conclusion of summing up the elements of the second row: $1+2+3+4+5+6=21$.

One of the properties of this table is each entrance in the diagonal beginning $\{i, j, \ldots\}$ reports the number of terms in the expansion of $(a_1 + a_2 + a_3 + \ldots + a_{n+3-j})^n$ for $n \geq j-2$. For instance, diagonal $\{1, 3, 10, 35, 126, \}$ means the number of terms in the expansion of $(a_1 + a_2 + a_3 + \ldots + a_{n-1})^n$, for $n \geq 2$, which is $\binom{2n-2}{n-2}$. Obviously, one can be obtained the sequence of Catalans numbers by dividing each term of this diagonal by 1, 2, 3, 4, ..., respectively.

The ith row of antidiagonals in Table 2 is equivalent to the i th row of the classical Pascal triangle. The term $a_{i,j}$ of Table 2 satisfies $a_{i,j} = a_{i-1,j} + a_{i,j-1}$. The determinants of matrices generated by the term $a_{1,1}$ are equal to 1. Also, the square matrices obtained from the term $a_{1,1}$ are symmetric in accordance with the diagonal $\{1, 2, 6, 20, 70, \}$.

As well as, if in 2 each row is moved two places to the right according to the prior row, Table 3 existed.

Take into account each column of Table 3 is equal to the corresponding diagonal of the Pascal 3-triangle which is also known as the "deformed" Pascal triangle [10].

Table 2
Number of paths between x-points and a y-points.

X	Y							
	0	1	2	3	4	5	6	7
0	1	1	1	1	1	1	1	1
1	1	2	3	4	5	6	7	8
2	1	3	6	10	15	21	28	36
3	1	4	10	20	35	56	84	120
4	1	5	15	35	70	126	210	330
5	1	6	21	56	126	252	462	792
6	1	7	28	84	210	462	924	1716
7	1	8	36	120	330	792	1716	3432
8	1	9	45	165	495	1287	3003	6435
9	1	10	55	220	715	2002	5005	11440

Table 3
Rectangular Pascal 3-triangle.

1	1	1	1	1	1	1	1	1	1	1	1
		1	2	3	4	5	6	7	8	9	10
				1	3	6	10	15	21	28	36
						1	4	10	20	35	56
								1	5	15	35
										1	6

6.1. Some properties of the pascal 3-triangle diagonals

It will be called here triple diagonal to each of the different lines of triples of contiguous numbers on the Pascal 3-triangle as shown in Table 1, from right to left and the from first row to bottom. For instance, the second triple diagonal is $\{1-3-6, 10-15-21, \}$ these lines are also called anti-diagonals.

It is clear that the n th diagonal terms of the Pascal 3-triangle are definitely the coefficients of the Taylor expansion of function $g_n(x) = \frac{1}{(1-x)^n}$ centered at the origin.

For a small value $x = 10^{-r}$ $(r \in \mathbf{N})$, when the function $g_n(x)$ written as a decimal number has its integer part equal to 1, and its decimal number can be seen as r-uplas showing the first terms of the n th antidiagonal of the Pascal 3-triangle. For instance,

$$g_5(10^{-3}) = \frac{1}{(1-10^{-3})^5} = 1.005015035070 \quad \ldots \to \{1, 5, 15, 35, 70, \ldots\}$$

which are the fifth anti-diagonal terms of the Pascal 3-triangle. Some characteristic properties of the Pascal 3-triangle are as follow:

1. The second diagonal is positive integer numbers. The third and fourth diagonal equal to the triangular and tetrahedral numbers, respectively. In general, i th diagonal equal to the $(i-1)$-dimensional simplex number [11].

2.Each element is obtained as a sum of the preceding elements in the same row and the previous element in the preceding diagonal.

3. The sum of the consecutive terms in the third diagonal is a perfect square.

4. By subtracting the odd number sequence from the triangular number sequence, the triangular number sequence is obtained again.

5. The n th element of the i th anti-diagonal denoted by $A_r(n)$. Then $\binom{A_r(n)=n+r-2}{r-1}$ here $(r-1)$ is $(i-1)$ th anti-diagonal.

6.2. Properties of the rows the pascal 3-triangle

Some properties of the Pascal 3-triangle rows are as follow:

1. The sum of the elements of the i th row is equal to the i th term of Narayana sequence.

2. The sum of the i th row elements and the $(i+1)$ th row elements is the corresponding $\{2, 2, 3, 5, 7, 10, 15, 22, 32, 47, 69, \}$ which are on OEIS, as A097333 and A058278 in http://oesis.org

3. Beginning with 1 on the left, and writing down the following number on its right in the immediately lower row, and so on the classical Pascal triangle is obtained.

7. Expression of k^n as a k-Narayana number

Firstly, the equations for the k-Narayana number is written in matrix form as follow

$$N = B \cdot K$$

. Here, $N = (N_{k,1}, N_{k,2}, N_{k,3}, .)^T, K = (1, k, k^2, k^3, \ldots)^T$ and B is the lower triangular matrix with elements the coefficients appearing in the expansion of the k-Narayana number in increasing powers of k:

$$B = \begin{pmatrix} 1 & & & & & & & & \\ 0 & 1 & & & & & & & \\ 0 & 0 & 1 & & & & & & \\ 1 & 0 & 0 & 1 & & & & & \\ 0 & 2 & 0 & 0 & 1 & & & & \\ 0 & 0 & 3 & 0 & 0 & 1 & & & \\ 1 & 0 & 0 & 4 & 0 & 0 & 1 & & \\ 0 & 3 & 0 & 0 & 5 & 0 & 0 & 1 & \\ 0 & 0 & 6 & 0 & 0 & 6 & 0 & 0 & 1 \\ 1 & 0 & 0 & 10 & 0 & 0 & 7 & 0 & 0 \end{pmatrix}$$

It is clear that the non-zero elements in matrix B are the same as the terms in the diagonals of the Pascal triangle. The sum of the elements of i th row is equal to the i th term of the classical Narayana sequence. Furthermore, the inverse of matrix B is

$$B^{-1} = \begin{pmatrix} 1 & & & & & & & & \\ 0 & 1 & & & & & & & \\ 0 & 0 & 1 & & & & & & \\ -1 & 0 & 0 & 1 & & & & & \\ 0 & -2 & 0 & 0 & 1 & & & & \\ 0 & 0 & -3 & 0 & 0 & 1 & & & \\ 3 & 0 & 0 & -4 & 0 & 0 & 1 & & \\ 0 & 7 & 0 & 0 & -5 & 0 & 0 & 1 & \\ 0 & 0 & 12 & 0 & 0 & -6 & 0 & 0 & 1 \end{pmatrix}.$$

Also, it is clear that k^n is equal to a linear combination of k-Narayana number:

$1 = N_{k,1}$
$k = N_{k,2}$

$k^2 = N_{k,3}$
$k^3 = N_{k,4} - N_{k,1}$
$k^4 = N_{k,5} - 2N_{k,2}$
$k^5 = N_{k,6} - 3N_{k,3}$
$k^6 = N_{k,7} - 4N_{k,4} - 3N_{k,1}$
$k^7 = N_{k,8} - 5N_{k,5} + 7N_{k,2}$
$k^8 = N_{k,9} - 6N_{k,6} + 12N_{k,3}$

8. Catalan transform of the *k*-Narayana sequence

Catalan number

For $n \geq 0$, the n th Catalan number is showed by [12].

$$C_n = \frac{1}{n+1}\binom{2n}{n} \quad \text{or} \quad C_n = \frac{(2n)!}{(n+1)!n!}$$

For some n, the first Catalan numbers are

$\{1, 1, 2, 5, 14, 42, 132, 429, 1430, 4862, 16796, \ldots\}$

From now on OEIS, as A000108 in http://en.wikipedia.org/wiki/Catalan number.

Following [13,14], we define the Catalan transform of the *k*-Narayana sequence as $\{N_{k,n}\}$

$$CN_{k,n} = \sum_{i=1}^{n} \frac{i}{2n-i}\binom{2n-i}{n-i} N_{k,i}, \quad \text{for} \quad n \geq 1 \quad \text{with} \quad CN_{k,0} = 0$$

We can give some members of Catalan transform of the first *k*-Narayana number. These are the polynomials in *k*:

$$CN_{k,1} = \sum_{i=1}^{1} \frac{i}{2-i}\binom{2-i}{1-i} N_{k,i} = 1$$

$$CN_{k,2} = \sum_{i=1}^{2} \frac{i}{4-i}\binom{4-i}{2-i} N_{k,i} = 1 + k$$

$$CN_{k,3} = \sum_{i=1}^{3} \frac{i}{6-i}\binom{6-i}{3-i} N_{k,i} = k^2 + 2k + 2$$

$$CN_{k,4} = \sum_{i=1}^{4} \frac{i}{8-i}\binom{8-i}{4-i} N_{k,i} = k^3 + 3k^2 + 5k + 6$$

$$CN_{k,5} = \sum_{i=1}^{5} \frac{i}{10-i}\binom{10-i}{5-i} N_{k,i} = k^4 + 4k^3 + 9k^2 + 14k + 18$$

$$CN_{k,6} = \sum_{i=1}^{6} \frac{i}{12-i}\binom{12-i}{6-i} N_{k,i} = k^5 + 5k^4 + 14k^3 + 31k^2 + 52k + 56$$

We can show $\{N_{k,n}\}$ as the $n \times 1$ matrix N_k and the product of the lower triangular matrix C as

$$\begin{pmatrix} CN_{k,1} \\ CN_{k,2} \\ CN_{k,3} \\ CN_{k,4} \\ \cdots \end{pmatrix} = \begin{pmatrix} 1 & & & & \\ 1 & 1 & & & \\ 2 & 2 & 1 & & \\ 5 & 5 & 5 & 3 & \\ \cdots & \cdots & \cdots & \cdots & \cdots \end{pmatrix} \begin{pmatrix} N_{k,1} \\ N_{k,2} \\ N_{k,3} \\ N_{k,4} \\ \cdots \end{pmatrix} = \begin{pmatrix} 1 \\ 1+k \\ k^2+2k+2 \\ k^3+3k^2+5k+6 \\ \cdots \end{pmatrix}$$

$$= \begin{pmatrix} 1 & & & & \\ 1 & 1 & & & \\ 2 & 2 & 1 & & \\ 5 & 5 & 5 & 3 & \\ \cdots & \cdots & \cdots & \cdots & \cdots \end{pmatrix} \begin{pmatrix} 1 \\ k \\ k^2 \\ k^3+1 \\ \cdots \end{pmatrix}$$

where

$C_{i,j} = \sum_{i=j-1}^{i-1} C_{i-1,r}$.

The lower triangular matrix $C_{n,n-i}$ is known as the Catalan triangle and its elements verify the formula

$C_{n,n-i} = \frac{(2n-i)!(i+1)}{(n-i)!(n+1)!}$ with $0 \leq i \leq n$.

9. Hankel transform

Let $A = \{a_0, a_1, a_2, \ldots\}$ be a sequence of real numbers [12]. The Hankel transform of A is the sequence of determinants $H_n = Det[a_{i+j-2}]$, i.e.

$$H_n = \begin{pmatrix} a_0 & a_1 & a_2 & a_3 & \ldots \\ a_1 & a_2 & a_3 & a_4 & \ldots \\ a_2 & a_3 & a_4 & a_5 & \ldots \\ a_3 & a_4 & a_5 & a_6 & \ldots \\ \ldots & \ldots & \ldots & \ldots & \ldots \end{pmatrix}.$$

The upper-left $n \times n$ subdeterminant of H_n is called the Hankel determinant of order n of sequence A. The Hankel transform of the Catalan sequence is the sequence $\{1, 1, 1, \}$ [15]. In [16], it is shown that the Hankel transform of the sum of consecutive generalized Catalan numbers is equal to the bisection of the Fibonacci sequence.

Considering the Catalan transform of the k-Narayana sequence, we get:

$$HCN_{k,1} = Det[1] = 1$$

$$HCN_{k,2} = \begin{vmatrix} 1 & 1+k \\ 1+k & k^2+2k+2 \end{vmatrix} = 1$$

$$HCN_{k,3} = \begin{vmatrix} 1 & 1+k & k^2+2k+2 \\ 1+k & k^2+2k+2 & k^3+3k^2+5k+6 \\ k^2+2k+2 & k^3+3k^2+5k+6 & k^4+4k^3+9k^2+14k+18 \end{vmatrix} = -2k-2$$

10. Conclusion

Flip graphs as well as cycles in sequences of Pascal 3-triangles reveal the inherent self-similarities in Narayana sequences. For conciseness, Betti numbers are introduced to simplify the characterization of the free group structures underlying Pascal 3-triangle cycles. In addition, we give some properties and theorems related to the *k*-Narayana numbers and show Cassinis identity and limit of the *k*-Narayana sequence. We also calculate the determinant of the *k*-Narayana numbers and show that their determinant are fixed terms.

Also, we give the sum of the first terms of the *k*-Narayana sequence and we deduce many properties of the *k*-Narayana numbers and related Pascal 3-triangle. In addition, we give an expression of the k^n as a *k*-Narayana number. Finally, we give the $CN_{k,n}$ description of the Catalan transformation of *k*-Narayana $N_{k,n}$ sequences. Furthermore, we write $CN_{k,n}$ transformation as the product of the Catalan matrix C, which is the lower triangular matrix and the N_k matrix of $n \times 1$ type. We calculate determinants of matrices which are formed with $CN_{k,n}$ by using the Hankel transform. These identities can be used to develop new identities of sequences.

Credit Author Statement

In this paper, E. Ozkan, B. Kuloglu have introduced the theory and structure of Narayana sequences, B. Kuloglu introduced the 2D and 3D geometric representations of Narayana sequences, J.F. Peters introduced flip graphs and free groups as means of visualizing oscillations in the growth and decline of Narayana populations as well as simplifying references to the cyclic structure of Narayana sequences.

Declaration of Competing Interest

The authors of this paper have no competing interests.

Table A.4
Minimal Planar Cell Complexes .

Minimal Complex	Cell $e^n : n \in \{0,1,2\}$	Planar Geometry	Interior
	e^0	Vertex	nonempty
	e^1	Edge	line segment w/o end points
	e^2	Filled triangle	nonempty triangle interior w/o edges

Acknowledgements

We extend our thanks to the anonymous reviewers for their helpful suggestions and comments.

This research has been supported by the Natural Sciences & Engineering Research Council of Canada (NSERC) discovery grant 185,986 and Instituto Nazionale di Alta Matematica (INdAM) Francesco Severi, Gruppo Nazionale per le Strutture Algebriche, Geometriche e Loro Applicazioni grant 9 920160 000362, n.prot U 2016/000036 and Scientific and Technological Research Council of Turkey (TÜBİTAK) Scientific Human Resources Development (BIDEB) under grant no: 2221-1059B211301223.

Appendix A. Cell Complexes

A planar Whitehead cell complex K [17] (usually called a CW complex) is a collection of n-dimensional minimal cells $e^n_\alpha, n \in \{0,1,2\}$, *i.e.*,

$$K = \left\{e^n_\alpha \subset \mathbb{R}^2 : n \in \{0,1,2\}\right\}.$$

in the Euclidean plane π.

Definition 2. A cell subcomplex $\mathrm{sh}E := \{e^n_\alpha\} \in 2^K$ (**shape complex**) is a **closed subcomplex**, provided the subcomplex includes both a nonempty interior (denoted by $\mathrm{int}(e^n_\alpha)$) and its boundary (denoted by $\mathrm{bdy}(e^n_\alpha)$). In effect, sh$E$ is closed, provided

$$\mathrm{sh}E = \mathrm{int}(\mathrm{sh}E) \cup \mathrm{bdy}(\mathrm{sh}E) \text{ (\textbf{Closed subcomplex}).}$$

Let 2^π be the collection of all subsets in the Euclidean plane π. In the plane, a Whitehead **Closure-finite Weak (CW)** cell complex $K \in 2^\pi$ has two properties, namely,

- **C** A cell complex K is **closure-finite**, provided each cell $e^n_\alpha \in K$ is contained in a finite subcomplex of K. In addition, each cell $e^n_\alpha \in K$ has a finite number of immediate faces. One cell e^n_α is an **immediate face** of another cell e^m_α, provided $e^n_\alpha \cap e^m_\alpha \neq \emptyset$ [18] (also called a **common face** [19, p. 3]).
- **W** The plane π has a **weak topology** induced by cell complex K, *i.e.*, a subset $S \in 2^\pi$ is closed, if and only if $S \cap e^n_\alpha$ is also closed in e^n_α for each n, α [18, §5.3, p. 65].

A collection $K \in 2^\pi$ is called a **CW complex**, provided it has the closure-finite property and π has the weak topology property induced by K.

Minimal cell planar complexes are given in Table A.4.

Remark 5. Closure finite cell complexes with weak topology (briefly, CW complexes) were introduced by J.C.H. Whitehead [9], later formalized in [20]. In this work[1], a **cell complex** K (or complex) [20, §4, p. 221] is a Hausdorff space (union of disjoint open cells e, e^n, e^n_i) such that the closure of an n cell $e^n \in K$ (denoted by $\mathrm{cl}(e^n)$ is the image of a map $f : \sigma^n \to \mathrm{cl}(e^n)$, where σ^n is a fixed n-simplex and where the boundary $\mathrm{bdy}(e^n)$ (otherwise known as the **contour** of a complex) is defined by

$$\mathrm{bdy}(e^n) = \overbrace{f(\mathrm{bdy}(e^n)) = \mathrm{cl}(e^n) - \mathrm{int}(e^n)}^{\textbf{Complex contour} \to \textbf{closure } \mathrm{cl}(e^n) \textbf{ minus } Int(e^n) \textbf{ interior}}.$$

Notice that a subcomplex $X \subset K$ has the weak topology, since X is the union of a finite number intersections $X \cap \mathrm{cl}(e)$ for single cells $e \in K$ [20, §5, p. 223]. From a geometric perspective, a cell complex is a triangulation of the CW space K [9, p. 246].

Appendix B. Shape Complexes

A shape complex has two basic parts, namely, contour and interior, introduced in [21].

Definition 3. A **planar shape contour** of a shape complex sh$E$ (denoted by $\mathrm{bdy}(\mathrm{sh}\boldsymbol{E})$) is a simple, closed curve with no self-loops.

Each shape complex sh$E$ has a nonempty interior that excludes all points on the shape contour.

Definition 4Shape complex interior. .

$$\overbrace{\mathrm{int}(\mathrm{sh}\boldsymbol{E}) = \mathrm{sh}\boldsymbol{E} \setminus \mathrm{bdy}\boldsymbol{E}}^{\textbf{Set of points bounde, by } \mathrm{sh}E \textbf{ contour}}.$$

The fundamental parts of every shape complex are gathered together in the closure of a shape complex, definite using the Hausdorff distance [22] (see, also, [23, §23, p. 128]) between all points in a CW complex K and a shape sh$E$.

Definition 5. Closure of a planar shape sh$E$ (denoted by $\mathrm{cl}(\mathrm{sh}\boldsymbol{E})$) in a CW space K is defined by

$$\overbrace{\mathrm{cl}(\mathrm{sh}\boldsymbol{E}) = \textbf{inf}\,\{\boldsymbol{x} \in \boldsymbol{X} : \boldsymbol{D}(\boldsymbol{x}, \mathrm{sh}\boldsymbol{E}) = \boldsymbol{0}\}.}^{\textbf{Hausdorff distance } D(x,\mathrm{sh}E)=\inf\left\{\|x-p\| : p \in \mathrm{sh}E\right\}}$$

In other words, we have the closure of a planar shape sh$\boldsymbol{E}$ is a finite bounded region of the Euclidean plane such that

$$\overbrace{\mathrm{cl}(\mathrm{sh}\boldsymbol{E}) = \mathrm{bdy}(\mathrm{sh}\boldsymbol{E}) \cup \boldsymbol{Int}(\mathrm{sh}\boldsymbol{E}).}^{\mathrm{cl}(\mathrm{sh}E) \textbf{includes its contour \& its interior}}$$

Appendix C. Finite 1-cycles and their Free Group Presentation

Finite 1-cycles in a CW space and their cyclic group presentations [17], [24] are briefly considered in this section. In arriving at cyclic group presentation derived from Pascal 3-triangles, we first consider 1-cycles, filled 1-cycles and shape complexes in a CW space.

Definition 6. A **1-cycle** E (denoted by cyc$E$) in a CW space is a finite, nonempty collection of path-connected vertexes $\left\{e^0_i \in K : e^0_i, i \geq 1, \text{is a zero cell}\right\}$ on 1-cells (edges) with no end vertex.

[1] Here, we use $cl(e^n)$ (closure of a cell) and $\mathrm{bdy}(e^n)$ (contour of a cell) used in this paper, instead of Whitehead's $\bar{e^n}$ and $\partial(e^n)$.

Definition 7. A **filled 1-cycle** in a CW space is a 1-cycle cyc$E$ has a boundary bdy(cyc$E$) (called its **contour**) that is a simple, closed curve with a nonempty interior int(cyc$E$).

Definition 8. In a CW space K, a **shape complex** E (denoted by sh$E$) is a finite region of K bounded by a simple closed curve with nonempty interior.

Theorem 8. *Every filled 1-cycle in a CW complex K is a shape complex of K.*

Proof. Immediate from Def. 7 and Def. 8. □

We can select what is known as a generator vertex in each 1-cycle.

Definition 9. A generator vertex v_0 in a 1-cycle cyc$E$ is the first vertex at the beginning of every path leading to any other vertex in cyc$E$. Let |cyc$E$| be the number of vertexes in cyc$E$ and let the set $\langle v_0\rangle$ be defined [25, p. 21] by

$$\langle v_0\rangle = \{v \in \text{cyc}E : v = kv_0, k \in \{1, \ldots, |\text{cyc}E|\}\}.$$

Recall that a **finite group** G is a nonempty set equipped with an associative binary operation $\circ$ (denoted by $G(\circ)$) such that G has the following members:

identity e: $g \circ e = g$ for every $g \in G$.
inverse $-g$: $g \circ -g = e$ for every $g \in G$.

A group G is **Abelian**, provided $g \circ g' = g' \circ g$ for every $g, g' \in G$.

Definition 10. A finite Abelian group G with a generator element $v_0 \in G$ (denoted by $G(\langle v_0\rangle, \circ)$) is a **cyclic Abelian group**, provided

$$G = \{g \in G : g \in \langle v_0\rangle\}.$$

A cyclic group with p generators is denoted by $\mathbb{Z}_p$ [26].

Intuitively, every boundary of a cell complex is a cycle [26, §4.8, p. 104]. This intuition leads to the following useful Lemma.

Lemma 2. *Every finite 1-cycle in a CW space has a corresponding Abelian cyclic group.*

Proof. Let cyc$E$ be a 1-cycle in a CW space K and let v_0 be a vertex in cyc$E$. From Def. 6, cyc$E$ is path-connected. Let + be a forward move (traversal) of an edge between adjacent vertexes in cyc$E$ and let $v \in \langle v_0\rangle$, *i.e.*, $v = kv_0$. For each pair $v, v' \in$ cyc$E$, we have

$$v + v' = kv_0 + k'v_0 = (k + k')v_0 = (k' + k)v_0 = v + v'.$$

Consequently, + is Abelian. Similarly, it can be shown that + is associative. For every $v \in$ cyc$E$, there is a reverse move $-v$ (the additive inverse of v). Let $0v_0 \in \langle v_0\rangle$ represent 0 moves from v_0, *i.e.*, $0v_0 = v_0$. The element $0v_0$ serves as an identity element. For each $v = kv_0 \in \langle v_0\rangle$, we have

$$v + 0v_0 = kv_0 + 0v_0 = (k + 0)v_0 = kv_0 = v, \text{ and}$$
$$v - v = kv_0 - kv_0 = (k - k)v_0 = 0v_0 = v_0.$$

Hence, cyc$E(\langle v_0\rangle, +)$ is an Abelian cyclic group. □

From Lemma 2, we obtain the following result for shape contours defined by the boundary of a collection of nested cycles.

Theorem 9. *The contour of every planar shape complex in a CW space has a cyclic group presentation.*

Proof. Let cyc$E$ be a 1-cycle in a CW space K and let 2^K be the collection of all subsets of K. Further, let the mapping $f : 2^k \to 2^K$ be defined by

$$\begin{aligned} f(\text{cyc}E) &= \{kg : 0 \le k \le |cycE| \ \&\ g \in cycE\}(from\ Lemma 2) \\ &= G(\langle g\rangle, +) \\ &= \mathbb{Z}_1. \end{aligned}$$

Hence, *cycE* has a cyclic group presentation. □

From Theorem 9, we obtain the following result for shapes defined by a collection of path-connected vertexes in nested cycles, attached to each other to form a vortex. Recall that a free group has n generators, $n \ge 1$.

Theorem 10. *Every shape complex that is a collection of nested 1-cycles attached to each other pairwise via edges in a CW space, has a free group presentation.*

Proof. Let vor$E$ be a vortex, which is a collection n 1-cycles $\{cyc_iE, 1 \le i \le n\}$ attached to each other via edges in a CW space K and let 2^K be the collection of all subsets of K. Each 1-cycle cyc_iE has its distinguished vertex $g_i \in cycE_i$ that is a generator of a cyclic group. Further, let the mapping $f : 2^k \to 2^K$ be defined by

$$\begin{aligned} f(\text{vor}E) &= \{\{kg_i\} : 0 \le k \le |cycE_i| \ \&\ g_i \in cycE_i, 1 \le i \le n\} \text{ (from Lemma 2).} \\ &= G(\langle g_1, \ldots, g_n\rangle, +) \\ &= \mathbb{Z}_n. \end{aligned}$$

Hence, *vorE* has a free group presentation. □

Free Group Betti Numbers. Recall that a Betti number is a count of the number of generators of a free group [27, p.24]. Hence, by counting the generators of a free group, a Betti number provides a simplified means of referencing as well as characterizing the free group structure of the cycles in a Pascal-3 triangles view of a Narayana sequence.

From Observation, we arrive at the chief advantage in considering free group presentations of the cycles in Pascal 3-triangles, namely, Betti numbers as a simplified means of characterizing the complex cycles inherent in Pascal 3-triangles. Notice that in a more advanced setting, the traditional form of Betti numbers as counts of generators of free groups is replaced by average Betti numbers of induced subcomplexes in triangulations of manifolds introduced in 2020 by G. Codenotti, J. Spreer and F. Santos [28].

References

[1] Paṇḍita N.. Gaṇita kaumudī (sanscrit). 1356 A.D. Trans. by P. Singh in 1998,MR1739184.
[2] Ramirez J, Sirvent V. A note on the k-narayana sequence. Ann Math Inform 2015;45:91–105. MR3438816
[3] Edgar G. Measure, topology, and fractal geometry. New York: Springer; 2008. xvi+268 pp. ISBN: 978-0-387-74748-4,MR2356043
[4] Milich M. Kreise für planare matchings (German). TU Berlin; 2018. Bachelor thesis.
[5] Jennings R. Flip graphs. Ramat-Gan,Israel: Bar-Ilan University; 2020. Supervisors: R. Adin, Y. Roichman, arXiv:2012.09010
[6] Barry P. Generalized catalan numbers associated with a family of pascal-like triangles. J Integer Seq 2019;22(5):1–50. Art. 19.5.8,MR4008156
[7] Milich M, Mütze T, Pergel M. On flips in planar matchings. Discrete Appl Math 2021;289:427–45. MR4184338
[8] Naimpally S, Peters J. Topology with applications. topological spaces via near and far. Singapore: World Scientific; 2013. Xv + 277 pp, Amer. Math. Soc. MR3075111
[9] Whitehead J. Simplicial spaces, nuclei and m-groups. Proceedings of the London Math Soc 1939;45(4):243–327. MR1576810
[10] Stakhov A. The generalized golden proportions, a new theory of real numbers, and ternary mirror-symmetrical arithmetic. Chaos, Solitons and Fractals 2007;33(2):315–34. MR2313546
[11] Graham R, Knuth D, Patashnik O. Matematyka konkretna. (polish) [Concrete mathematics]. Warsaw,Reading, MA: Wydawnictwo Naukowe PWN,Addison Wesley; 1998. 719 pp., ISBN: 83-01-12124-6 68-01, MR1678922
[12] Barry P. A catalan transform and related transformations on integer sequences. J Integer Seq 2005;8(4):1–24. MR2165334
[13] Cvetković A, Rajković R, Ivković M. Catalan numbers, and hankel transform and fibonacci numbers. J Integer Seq 2002;5(1):1–8. .1.3,MR1919940
[14] Tastan M, Özkan E. Catalan transform of the k-jacobsthal sequence. Electron J Math Anal Appl 2020;8(2):720–74. ISSN: 2090-729X,MR4087829
[15] Sloane N. The on-line encyclopedia of integer sequences. Annales Mathematicae et Informaticae 2020. MR3822822

[16] Rajković P, Petković M, Barry P. The hankel transform of the sum of consecutive generalized catalan numbers. Integral Transforms Spec Funct 2007;18(3–4):70–4. MR2319589
[17] Peters J. Computational geometry, topology and physics of digital images with applications. shape complexes, optical vortex nerves and proximities. Cham, Switzerlan: Springer Nature; 2020. xxv+440 pp.,ISBN 978-3-030-22191-1/hbk; 978-3-030-22192-8/ebook, MR4245153, Zbl07098311, reviewed by K. Gdawiec (Sosnowiec)
[18] Switzer R. Algebraic topology – homology and homotopy. Berlin: Springer; 2002. xii+526 pp., Zbl 1003.55002
[19] Öztun S, Bildik N, Mutlu A. The construction of simplicial groups in digital images. J Inequal Appl 2013;2013:143:351–6. MR3055827
[20] Whitehead J. Combinatorial homotopy. i. Bull Amer Math Soc 1949;55(3):213–45. MR0030759
[21] Peters J. Proximal planar shapes. correspondence between triangulated shapes and nerve complexes. Bulletin of the Allahabad Mathematical Society 2018;33:113–37. MR3793556, Zbl 06937935, Review by D. Leseberg (Berlin)
[22] Hausdorff F. Grundzüge der mengenlehre. Leipzig: Veit and Company; 1914. Viii + 476 pp.
[23] Hausdorff F. Set theory, trans. by j.r. aumann. Providence, RI: AMS Chelsea Publishing; 1957. 352 pp.
[24] Cattabriga A, Mulazzani M. Strongly-cyclic branched coverings of (1,1)-knots and cyclic presentations of groups. Math Proc Cambridge Philos Soc 2003;135(1):137–46. MR1990837
[25] Rotman J. The theory of groups. an introduction. fourth edition. New York: Springer-Verlag; 1965, 1995. xvi+513 pp. ISBN: 0-387-94285-8, MR1307623
[26] Giblin P. Graphs, surfaces and homology, 3rd ed. Cambridge, GB: Cambridge University Press; 2016. Xx+251 pp. ISBN: 978-0-521-15405-5, MR2722281, first edition in 1981, MR0643363
[27] Munkres J. Elements of algebraic topology, 2^{nd} ed. Cambridge, MA: Perseus Publishing; 1984. ix + 484 pp., ISBN: 0-201-04586-9, MR0755006
[28] Codenotti G, Spreer J, Santos F. Average betti numbers of induced subcomplexes in triangulations of manifolds. Electron J Combin 2020;27(3):40pp.. MR4245153